TRANSIENT SPATIOTEMPORAL CHAOS ON COMPLEX NETWORKS

By

Safia Rawoot

RECOMMENDED:

Advisory Committee Chair

Chair, Department of Physics

APPROVED:

Dean, College of Natural Science and Mathematics

Dean of the Graduate School

December 16, 2004

Date

TRANSIENT SPATIOTEMPORAL CHAOS ON COMPLEX NETWORKS

A

THESIS

Presented to the Faculty

of the University of Alaska Fairbanks

in Partial Fulfillment of the Requirements

for the Degree of

MASTER OF SCIENCE

By

Safia Rawoot, B.S.

Fairbanks, Alaska

December 2004

Abstract

Some of today's most important questions regard complex dynamical systems with many interacting components. Network models provide a means to gain insight into such systems. This thesis focuses on a network model based upon the Gray-Scott cubic autocatalytic reaction-diffusion system that manifests transient spatiotemporal chaos. Motivated by recent studies on the small-world topology discovered by Watts and Strogatz, the network's original regular ring topology was modified by the addition of a few irregular connections. The effects of these added connections on the system's transience as well on the dynamics local to the added connections were examined. It was found that the addition of a single connection can significantly effect the transient time of spatiotemporal chaos and that the addition of two connections can transform the system's spatiotemporal chaos from transient to asymptotic. These findings suggest that small modifications to a network's topology can greatly affect its behavior.

Table of Contents

List of Figures

Acknowledgements

First I would like to thank my adviser Renate without whose support I would likely not have returned to the university much less finished this thesis. Furthermore, I am deeply grateful for the endless hours she has invested in this work.

Thanks to the members of my committee as well the other members of the Turbulence and Complex systems research group, my teachers and fellow graduates students for their valuable input and many good conversations.

Thanks also to Mary Parsons for all of the small ways she has made my life here at the university better.

I am grateful to my family for all of their help and support. I owe them more than I could ever repay.

Finally, thank you to my husband for everything.

Chapter 1

Introduction

Traditionally, physical science has sought to understand the world by reducing it to its most fundamental constituents. There are many real systems, however, where an understanding of the constituent parts is insufficient to explain their collective behavior – a complete understanding of the hydrogen atom gives almost no insight into the temperature or pressure of hydrogen gas nor does any amount of acquaintance with a single ant suggest the impressive structure of an ant colony. In both of these examples an understanding of the interactions between the system's constituent parts is additionally required to explain the system's emergent properties. Increasingly, studies are focusing on the effects of the interactions in dynamical systems and the complex behavior that emerges from their interconnected parts [1, 2, 3]. In the same vein, this thesis focuses on a system where a chaotic pattern emerges in a network of non-chaotic coupled dynamical components. The effects of increasing the complexity of the network's topology on this emergent dynamics is explored.

In the context of this thesis *"dynamical system"* simply refers to a system whose state changes deterministically in time. That is, the initial state of the system determines all of its future states. Governing equations transform or *map* old values of the system's state variables into new ones generating the system's evolution in time. The successive values of a system's state variables is know as its trajectory.

Chaos is the term given to a type of aperiodic, complex dynamics that can arise in nonlinear systems. Though chaotic systems are entirely deterministic, their behavior appears erratic and unpredictable. The conditions under which deterministic chaos can arise and

associated universal rules have been the subject of much research. Chaos in low-dimensional mathematical models and experimental systems is now well understood [4, 1].

Mathematical models that give rise to chaos provide a rich opportunity to study this complicated behavior in relatively simple systems [1]. The logistic map, one such well studied and perhaps familiar model, exemplifies some important signatures of chaotic behavior. The logistic map is defined by a one-dimensional quadratic difference equation that describes the growth of a single biological population under resource competition:

$$x_{t+1} = ax_t(1 - x_t) \tag{1.1}$$

Despite its simplicity, for certain values of the parameter a the logistic map describes a population that fluctuates chaotically in time [4, 5]. Two chaotic time series with slightly different initial states both generated using the logistic map and $a = 4$ are pictured in Fig. 1.1.

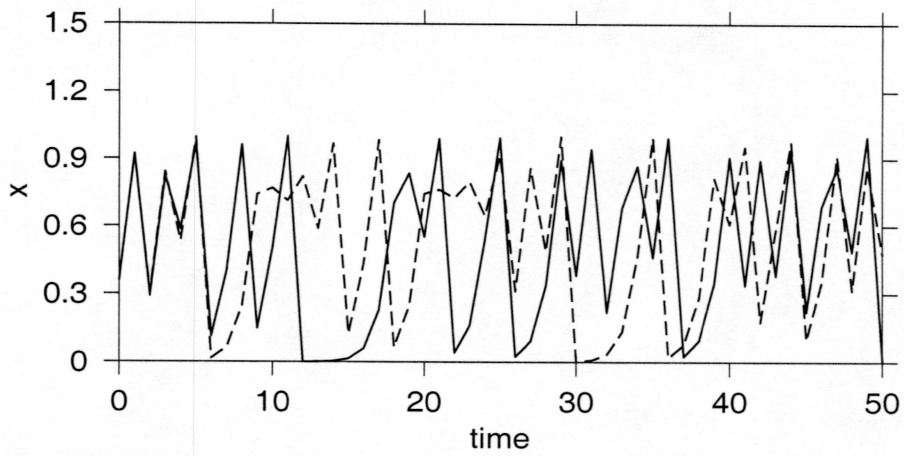

Figure 1.1. **The logistic map.** Chaotic time series generated by the logistic map with $a = 4$. For the solid line $x_0 = 0.4$ and for the dashed line $x_0 = 0.4001$.

Aperiodicity is the first important feature of chaotic behavior these time series illustrate. It is well established that time series generated by the logistic map with this parameter value do not repeat [4, 5]. The second feature is the sensitivity of chaotic systems to initial conditions. The two systems pictured in Fig. 1.1 were started in very similar states; by the tenth iteration, however, it can be seen that the two time series bear no resemblance.

Though the chaotic trajectories are required to be bound (for the logistic map $0 \leq x_t \leq 1$), nearby trajectories diverge from each other exponentially. This exponential divergence of trajectories in a chaotic system is quantified by a parameter called the Lyapunov exponent [4, 5].

The system discussed in this thesis is a network of many coupled iterated maps based on the Gray-Scott model for an open autocalytic reaction [6]. Like the logistic map, these equations also model a simple predator-prey interaction. Coupling many of these maps into a spatially distributed system results in chaotic fluctuations of the predator and prey population in time and space [7]. The spatiotemporal chaos that arises from the interactions in such high dimensional or spatially distributed systems is only beginning to be explored [7, 2, 1]. Further complicating the dynamical behavior of the system under study is the transience of its chaos. The system's chaotic dynamics collapses into a steady state with the sudden global extinction of the predator species. This extinction is not precipitated by any external perturbation, it is inherent to the dynamics of the system [8]. This startling phenomenon arising from a simple mathematical model has actually been proposed as a possible mechanism for observed extinctions in ecological systems where no external cause was evident [9, 10].

Understanding how the connections between dynamical components affect this system's collective dynamics is the central goal of this thesis. The abstraction of a network as a collection of entities, referred to here as nodes, and the connections between them, therefore provides a suitable framework on which to explore the system. A brief discussion of network topologies follows.

The variety of network topologies in natural systems is vast and ranges from almost complete order to apparent randomness. The purely structural aspects of networks at these two extremes of order and randomness have long been studied and are well understood [1]. Examples of a regular and random network are depicted in Fig. 1.2. Regular networks are characterized by coherent *neighborhoods* whose nodes are more likely to be connected to each other than they are to more distant nodes. Such organization is only found by chance in random networks. The *characteristic path length*, or the average number of connections between any two nodes in a network, is longer for a regular network than it is for a totally random network with the same number of nodes and connections [3]. This is due to the

possibility of long-range (as opposed to nearest neighbor) connections in random networks.

Between the topological extremes of regularity and randomness falls the structure of *small-world* networks – the subject of much recent exploration. This sort of topology, first discovered by Watts and Strogatz [3], is predominantly regular but with a few interspersed long-range connections. These few long-range connections are all that is required to drastically shorten the characteristic path length from that of a comparable regular network. An example of a small-world network is also shown in Fig. 1.2.

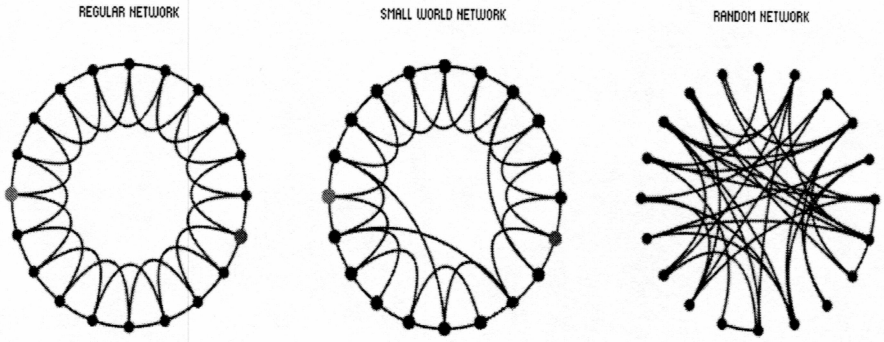

Figure 1.2. **Three network topologies.** [1]

Though these descriptions are useful, networks in the natural world are not merely static pieces of architecture but are the backbone of dynamical systems. Each component entity in even man-made systems has its own complex behavior.

Historically, most work on extended nonlinear dynamics, including previous studies of the Gray-Scott model, focused on systems whose connections have simple geometric architecture allowing dynamical intricacies to be more easily explored [7, 8, 1]. The structure of many real systems does have a coherency that is well suited to such a geometric description – for example any system where interactions are mediated via uniform diffusion. There are, however, many other situations that arise in nature where interactions do not occur in this regular way [1].

Recent studies focusing on small-world topology have begun to bridge the gap between structurally simple network models and the complexities of the natural world. The wiring

diagram for a surprising number of real-world networks, from an even more surprising variety of contexts seems to conform to this pattern of regularity punctuated by a few irregular connections [3]. The observation that the chain of acquaintances linking any two people on earth is on average quite small, known popularly as "six degrees of separation," is a consequence of the supposed small-world structure of social networks. Only a few well connected people can knit a large society. Some structurally quantifiable social networks have proved themselves to be definitely small-worlds – for example, the network of film actors where the actors themselves are the nodes and where two having worked together in a film constitutes a connection. In addition to social networks, for example, the neural network of the nematode earthworm *C. elegans*, as well as power transmission grids all show characteristics of a small-world topology.

Studies have begun to uncover the effects of small-world topology on dynamical systems. A small-world network of coupled phase oscillators was shown to synchronize almost as readily as if each oscillator had been connected to every other in the system – despite many orders of magnitude fewer connections [3]. Recently, a study has shown that the addition of random shortcuts to a network of chaotic oscillators to form a small-world topology can even transform the chaotic spatiotemporal dynamics to periodicity [2].

In the following chapters the effects of small-world inspired topologies on the dynamics of the network under study will be examined. Chapter 2 introduces the mathematical model used in these studies. In Chap. 3, the effects of a single distant connection on the time before global extinction in an otherwise regularly connected system is discussed. Chapter 4 explores in detail the consequences of such an added connection on the local dynamics of a system yielding further understanding of the statistical results obtained in Chap. 3.

Chapter 2

Background

The mathematical model under study represents a collection of nodes connected into a ring network. The dynamics at each node is governed by a pair of coupled nonlinear equations. This network displays dynamical patterns which are complex and not yet fully understood.

2.1 Dynamics of an isolated node

The equations that govern the dynamics at a node (the system's *local dynamics*) are based on a model that was originally motivated by the following open autocatalytic chemical reaction [6]:

$$\begin{aligned} A + 2B &\rightarrow 3B, \\ B &\rightarrow C. \end{aligned} \tag{2.1}$$

The autocatalator B consumes a sustaining resource A and decays to a final product C. Generally, "open" signifies that the reaction receives input from an external reservoir. The reactant B can also be thought of as a predator species that consumes a prey species A (sometimes referred to as "food" or "resource"). Two members of the predator species ($2B$) reproduce to create a third ($3B$). The decay of B into the final product C reflects the predator's mortality. This reaction is modeled by the following coupled differential equations [7]:

$$\frac{da}{dt} = 1 - a - \mu a b^2,$$

$$\frac{db}{dt} = \mu a b^2 - \Phi b, \tag{2.2}$$

where a and b are the dimensionless concentrations of the resource A and species B, and Φ and μ are parameters determined by the rate constants for the reactions. The system is modeled such that B is only initially seeded into the system, whereas the food A is continually replenished to its maximal value (a=1) from the reservoir.

The uncoupled system has three steady-state solutions given below as $S = (a, b)$:

$$\begin{aligned} S^n &= (1, 0) \\ S^f &= ((1 - \sqrt{1 - 4\Phi^2/\mu})/2, (1 + \sqrt{1 - 4\Phi^2/\mu})/(2\Phi)) \\ S^s &= ((1 + \sqrt{1 - 4\Phi^2/\mu})/2, (1 - \sqrt{1 - 4\Phi^2/\mu})/(2\Phi)). \end{aligned} \tag{2.3}$$

Linear stability analysis shows that the state S^n, where the food is maximal ($a = 1$) and the predator species is extinct ($b = 0$), is a stable steady state for every value of the parameters Φ and μ. S^f and S^s are unstable steady states that only exist where $\mu \leq 4\Phi^2$. In the parameter region of interest, where $2 < \Phi < 4$ and $\mu < \Phi^4/(\Phi - 1)$, S^f is an unstable focus and S^s is a saddle point. These three stationary states determine the system's local dynamics [7].

Figure 2.1 shows a *phase portrait* of the dynamics at an isolated node. The two-dimensional Cartesian space where one axis is defined by a and the other by b is known as *phase space*. The path in phase space described by a node's state as it changes in time is called a *trajectory*.

Equation (2.2) represents an excitable system as is illustrated in Fig. 2.1. The trajectories start at the stable steady state when a perturbation is applied by the introduction of the predator species B. If the perturbation is below some threshold (i.e. a *sub-critical* perturbation), a node's trajectory will return immediately to the stable extinct state S^n, whereas if the perturbation is above some threshold (*super-critical*) it will make an excursion about the unstable focus S^f before returning to the stable steady state. This excitation is the primary process that drives the system's local dynamics even when the isolated nodes have been coupled into a network.

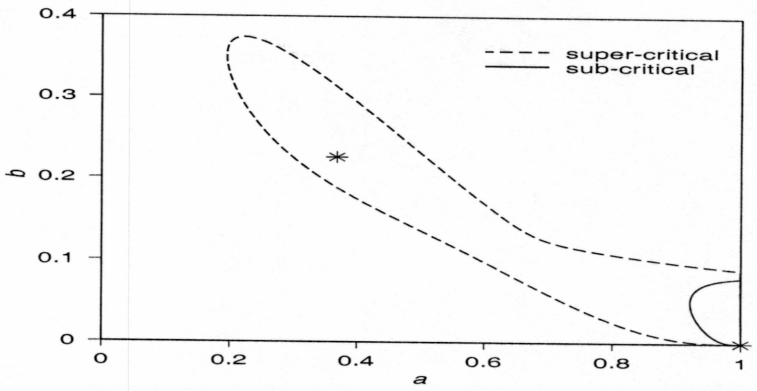

Figure 2.1. **Phase portraits for an isolated node, Eqn. (2.2).** The dimensionless concentrations a and b are plotted on the horizontal and vertical axes, respectively. The two steady states $S^n = (1, 0)$ and $S^f = (0.368, 0.225)$ with $\mu = 33.7$ and $\Phi = 2.8$ are marked. Equation (2.2) was integrated using the Euler method with a numerical time step $dt = 0.0003$.

2.2 The regularly connected ring network

The reaction dynamics from Eqn. (2.1) was originally modeled on a continuous reaction-diffusion system [7]. Here, though, the dynamics is modeled on a network of discrete, spatially coupled maps. All of the simulations in this study start with the network nodes coupled to their nearest neighbors and with periodic boundary conditions so that they form a regularly connected ring network (see Fig. 2.2). The governing equations for the *nth* node become:

$$\begin{aligned} \frac{da_n}{dt} &= 1 - a_n - \mu a_n b_n^2 + D([a_{n+1} - a_n] + [a_{n-1} - a_n]), \\ \frac{db_n}{dt} &= \mu a_n b_n^2 - \Phi b_n + D([b_{n+1} - b_n] + [b_{n-1} - b_n]), \\ n &= 1, 2, .., N. \end{aligned} \tag{2.4}$$

The added coupling terms in Eqn. (2.4) are a discrete version of the one-dimensional Laplacian operator, the coupling is therefore termed *diffusive*. Under the original reaction-diffusion interpretation, the parameter D contained information about the spatial discretization of the system and the diffusivity of the predator and prey concentrations. Under the current network interpretation D simply determines in part the coupling strength; for $D = 0$ the regularly coupled system reduces to a collection of isolated nodes each with dynamics

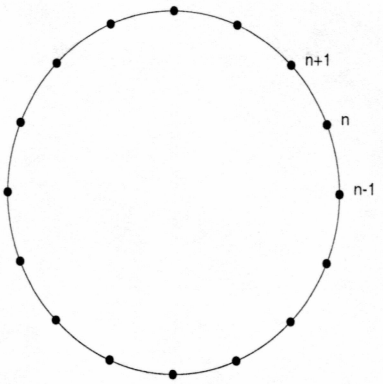

Figure 2.2. **Regularly connected ring network, Eqn. (2.4).** Each node is connected to only its two nearest neighbors.

described by Eqn. (2.2). The spatial-coupling is also proportional to the gradient between connected nodes. In the regularly connected system $D = 16$ a value consistent with that used in other studies [7, 8] . The network is excitable because its nodes are each excitable dynamical systems.

2.2.1 Local dynamics

Figure 2.3 shows a phase portrait for a representative node in the spatially-coupled system described by Eqn. (2.4). Nodal dynamics is still primarily governed by the steady state solutions (Eqns. (2.3)), even with the addition of diffusive coupling. Trajectories still return to the vicinity of the stable steady state S^n. Because of the coupling, however, the dynamics of a node is perturbed super-critically by the dynamics at its neighbors and so is re-excited into an orbit about the unstable focus. The super-critical perturbation of a single node can excite a propagating wave where the perturbation is transmitted from one node to the next throughout the network [7].

With the addition of the coupling terms a perturbation, or reaction-diffusion front, can propagate throughout the system. This reaction-diffusion wave connects the stable state S^n in front of the wave to the unstable focus S^f behind the wave (see Fig. 2.4). Nodes in the immediate wake of the wave have a and b values very close to the unstable focus S^f. As time proceeds the node's trajectories spiral away from S^f and eventually move toward S^n where, if the nodes were not spatially coupled, the reaction dynamics would collapse,

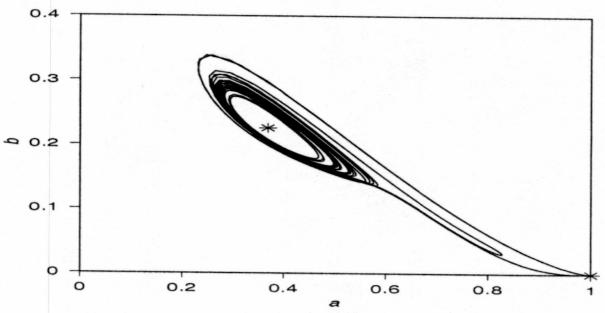

Figure 2.3. **Phase portrait for the dynamics of a representative node in a regularly connected ring network.** $S^n = (1, 0)$ and $S^f = (0.368, 0.225)$ are marked. Numerical integration of Eqn (2.4) and all other parameters are the same as in Fig. 2.1 with $N = 400$.

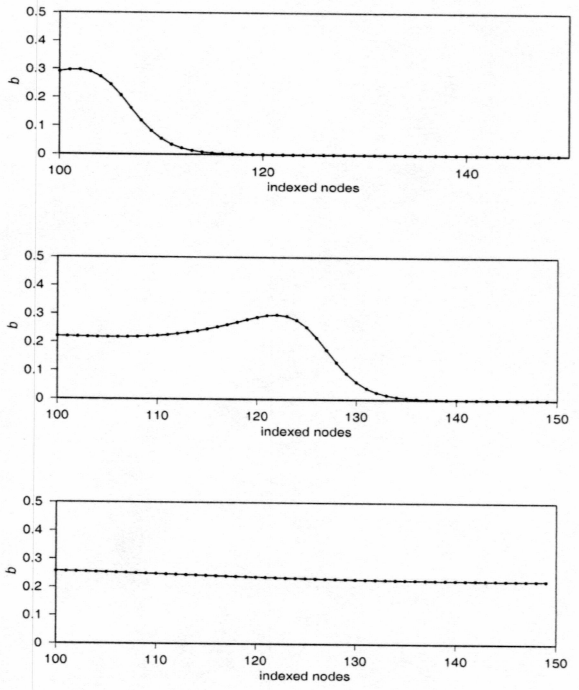

Figure 2.4. **A series of concentration profiles of species b at successive times.** Time proceeds from top to bottom. Each dot on the plot depicts the dynamics of a single node, the level of the node as measured on the vertical axis signifies the b value at that node. Each node is connected to the nodes immediately to its right and left, only a portion of the connected system is depicted. These images are from the same simulation used to generate Fig. 2.3.

i.e. the predator species would become extinct. Instead, because other nodes with a non-zero and super-critical b value can re-perturb neighboring nodes in the extinct state S^n, the system remains dynamical [1]. Put another way, in the parameter region where the unstable focus S^f exists, spatial coupling allows the predator to re-invade regions where it had formerly died out.

2.2.2 Global Dynamics

The spatiotemporal dynamics of the regularly connected network is shown in Fig. 2.7 at the end of the section. Initially, the concentration of food is maximal throughout the medium ($a = 1$). The initial invasion of the predator B is represented by the lines sloping from the point of its initial seeding. Nodes in the gray regions have a and b values in the vicinity of the unstable focus, S^f. The white patches show regions where the dynamics has returned to the stable extinct state S^n. The predator's re-invasion from either side of the local extinction causes the triangular shape of the white patches.

Studies have shown that the pattern in Fig. 2.7 bears the hallmarks of spatiotemporal chaos [7, 11]. The most common quantifier of chaos in a system is known as the *Lyapunov exponent* λ. The Lyapunov exponent describes a system's sensitivity to its initial conditions. In a chaotic system, λ is positive signifying that the trajectories of two systems initially in similar states will diverge exponentially. The Lyapunov exponent for the regularly connected Gray-Scott system [11] has been determined numerically to converge to a positive value (see Fig. 2.5). Chaos in a spatially distributed system (that is, spatiotemporal chaos) is additionally characterized by a rapid decay in spatial correlations. The correlation length calculated for this system is consistent with expectations for spatiotemporal chaos [7].

Spatiotemporal chaos in this system is not asymptotic, but transient [8]. Figure 2.8 at the end of the section shows the sudden onset of global extinction. The extinction occurs when all trajectories are so close to the stable state S^n such that there exists no super-critical perturbation in the system. Because the strength of the spatial coupling is dependent on the gradient between connected nodes (Eqn.(2.4)) the proximity of all of the system's trajectories causes them behave as if they were not coupled to each other at all. The system's trajectories all move to S^n following a path similar to the super-critical trajectory of an isolated node depicted in Fig. 2.1 thus causing complete collapse of the

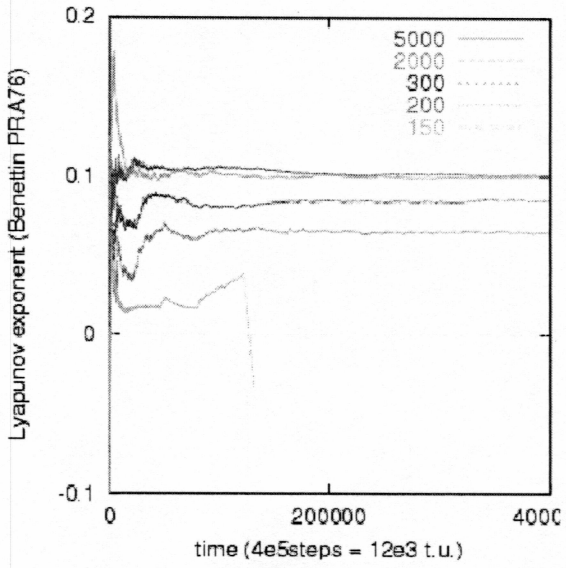

Figure 2.5. **Convergence of the finite Lyapunov exponent with time.** Calculation made at a representative regular network node with N=7000 [11].

system's dynamics. The time between the initial development of spatiotemporal chaos and its collapse (*transient time*) is, as of yet, impossible to predict a priori, and it varies greatly for different initial conditions. The average transient time for a set of random initial conditions depends exponentially on the size of the network (see Fig. 2.6). The reason for this dependence is yet to be uncovered [8].

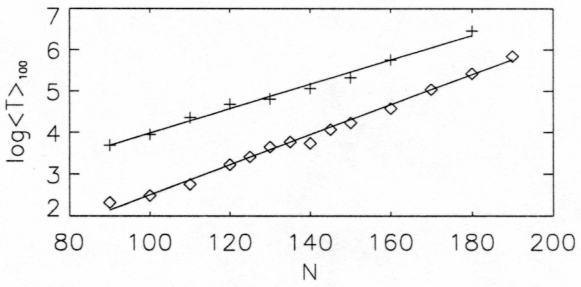

Figure 2.6. **Transient time T versus system size N.** Calculation made for 100 different initial conditions[8]. The solid line represents a robust line fit of the data.

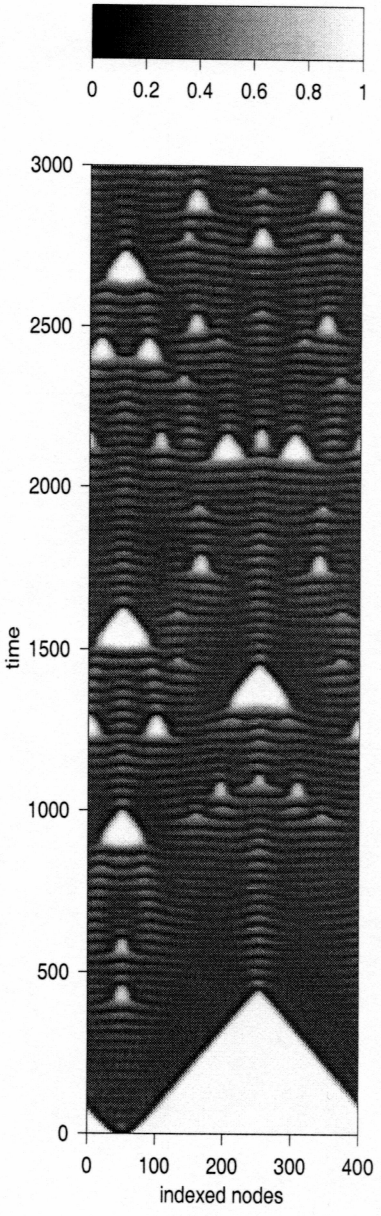

Figure 2.7. **Spatiotemporal dynamics for resource concentration a, Eqn. (2.4).** Each line of the spatiotemporal plot gives a snapshot of the entire system (temporal resolution is 0.15 time units). Because this is a ring-network, its right and left hand edges are actually connected, i.e. the boundary conditions are periodic. The gray-scale gives information about the quantity of food in the system, a. White signifies a is maximal, and black, that the value of a is zero. Generally white in the spatiotemporal plot implies a zero b value (i.e. the predator species is extinct) whereas the value of b increases roughly as gray darkens to black. All numerical and system parameters are the same as in Fig. 2.3.

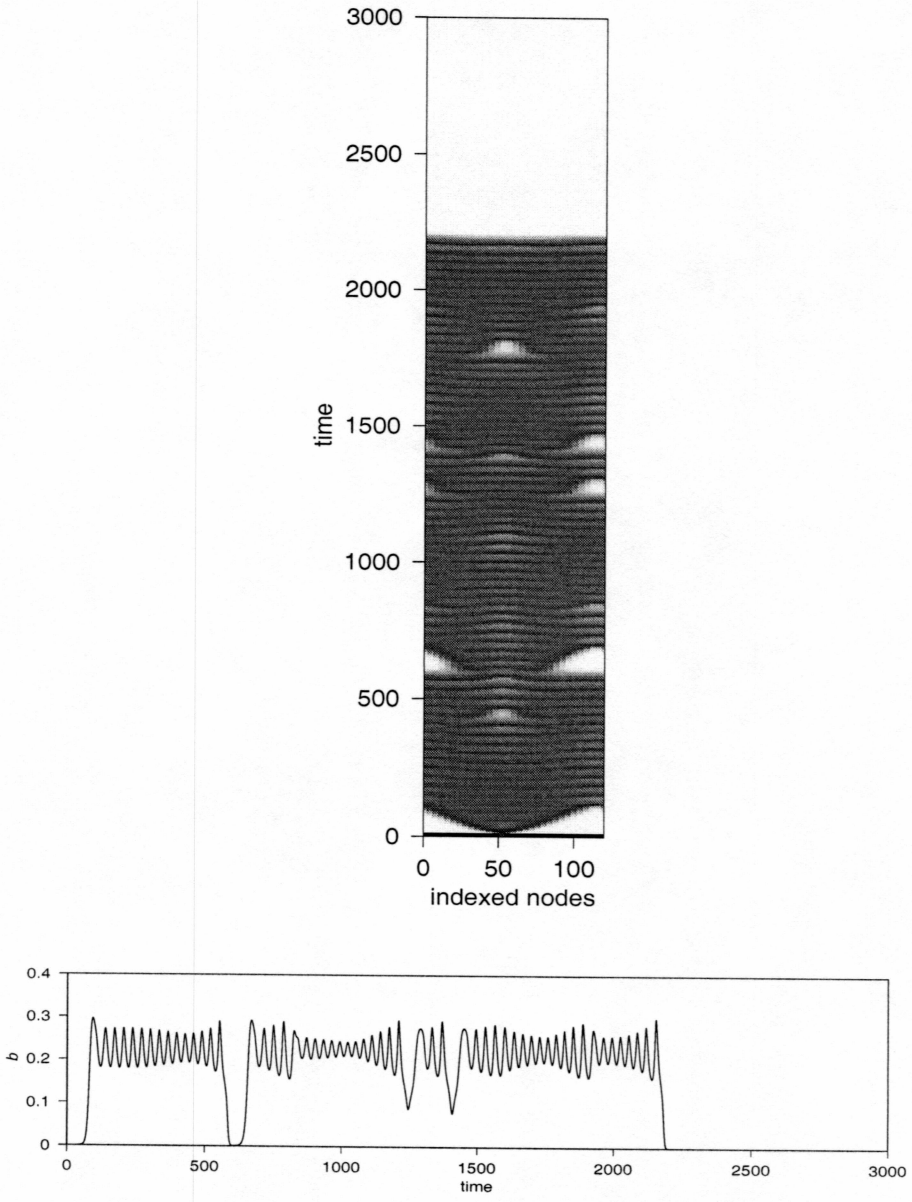

Figure 2.8. **Spatiotemporal dynamics for resource concentration a showing dynamical collapse of a regularly connected system (Eqn. (2.4)).** Calculated with $N = 120$ and all other numerical and system parameters as in Fig. 2.1. The time series of the species concentration b at a single node $n = 75$ is shown in the lower figure.

2.3 Adding shortcuts to a regularly connected ring network

The highly synchronous state of spatiotemporal chaos in a regularly connected system immediately prior to global extinction is not yet understood. The addition of shortcuts to the network is motivated by the enhanced synchronicity displayed in other networks with small-world coupling.

The regular ring network in Fig. 2.2 is manipulated by the addition of a shortcut between node n and another distant node m (Fig. 2.9). Consequently an additional coupling term is added to the dynamical equations for the nth node (Eqn. (2.4)) that accounts for the gradient between node n and m.

$$\begin{aligned} \frac{da_n}{dt} &= 1 - a_n - \mu a_n b_n^2 + D_n([a_{n+1} - a_n] + [a_{n-1} - a_n] + [a_m - a_n]), \\ \frac{db_n}{dt} &= \mu a_n b_n^2 - \Phi b_n + D_n([b_{n+1} - b_n] + [b_{n-1} - b_n] + [b_m - b_n]), \end{aligned} \tag{2.5}$$

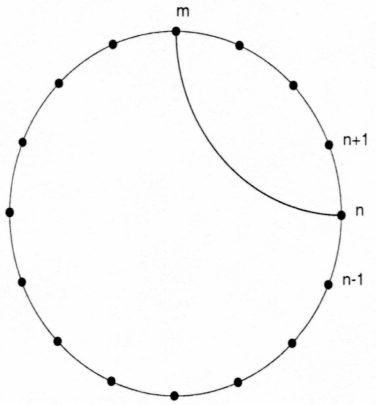

Figure 2.9. **Regularly connected network with a single added shortcut between node n and node m.** For this system $N = 16$ and the shortcut spans 4 nodes so shortcut length $s = 0.25$.

These equations describe the dynamics at the nth node. As before, the node is connected to both its nearest neighbors, and the additional term establishes a connection to the mth node. The diffusive coupling coefficient D (from Eqn. (2.4)) must be scaled by the number of connections made at each node so that $D_n = 2D/k_n$, where k_n is the number of connections to node n. This scaled D_n ensures that the average perturbation is the same at each node, independent of the number of connections made to it.

The length of a shortcut s is defined by the number of nodes the shortcut bypasses in the regular ring. The length s is scaled by the system's size so that for Fig. 2.9, where $N = 16$ and the shortcut spans 4 nodes, $s = 0.25$. The studies in the following chapters focus in detail on the effects of added shortcuts on a regularly connected system.

2.4 Summary

The interplay between the nodal dynamics described in Eqn. (2.2) and the diffusive coupling added in Eqn. (2.4) gives rise to transient spatiotemporal chaos in a regular network. Dynamical collapse is precipitated by the convergence of all the system's trajectories into the vicinity of the stable steady state S^n. To probe the robustness of synchronization and dynamical collapse in this system, the network topology is modified by the addition of shortcuts to the regularly connected ring (see Eqn. (2.5)).

Chapter 3

Transient Spatiotemporal Chaos in the Presence of One Shortcut

The addition of a few shortcuts to a regularly connected ring network can greatly affect its structural characteristics – one shortcut can cut the average number of connections between any two nodes in the system (characteristic path length) by 25 percent. Therefore, the simplest network manipulation is performed to gain insight into the response of the system's dynamics to increasing structural complexity.

The regular ring network (Eqn. (2.4)) was modified by the addition of a single shortcut between two nodes (Eqn. (2.5)). For a fixed shortcut length s, the average transient time of the spatiotemporal chaos was determined in one hundred manipulated systems each starting from a different randomly generated initial state. To exclude initial transient effects, the shortcut was made at a time late enough to ensure spatiotemporal chaos had fully developed. The average transient time was determined as a function of shortcut length s and compared to the control case with no shortcut ($s = 0$).

Figure 3.1 shows the ensemble's mean transient time T as a function of the shortcut length s. Between the control case where $s = 0$ and $s = 0.05$ there is a sharp increase in the average transient time for the ensemble T. For shortcuts with $s > 0.05$, T decreases with shortcut length s. T for the shortcut systems does not fall below T for the control case, though, until $s > 0.15$.

Since the collapse of spatiotemporal chaos is preceded by a synchronized state, the reduc-

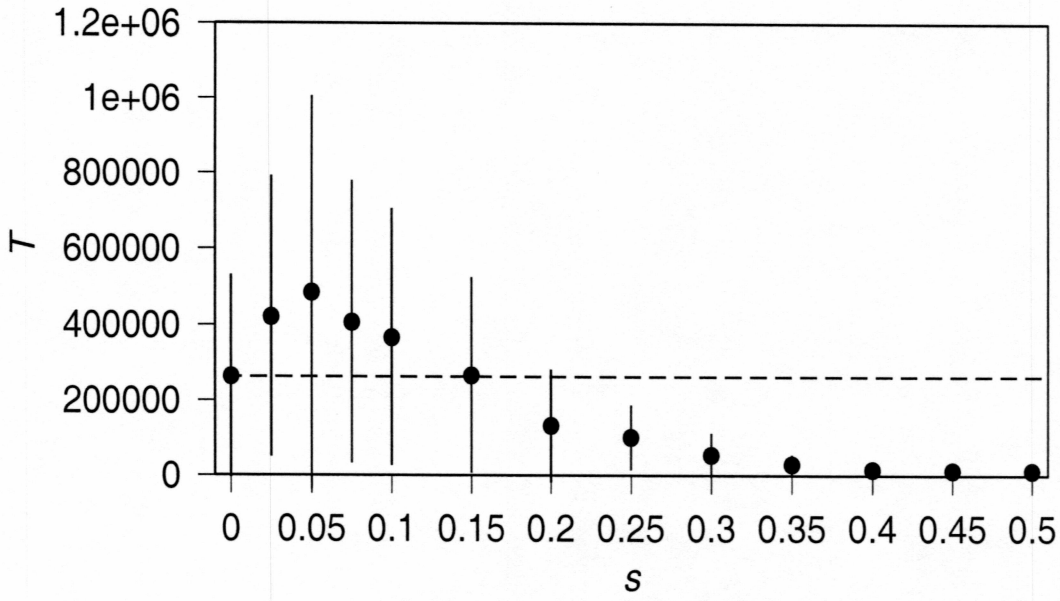

Figure 3.1. **Mean transient time T as a function of shortcut length s.** Simulations were performed for an ensemble of one hundred manipulated systems with randomly generated initial conditions with $N = 180$. Numerical and system parameters are the same as used for Fig. 2.1. An earlier study on the transient time of spatiotemporal chaos on regular networks showed that increasing the ensemble's size from 100 to 2000 only changed the mean transient time by 0.1 percent [8].

tion in the lifetime of the chaotic dynamics can be qualitatively explained by the shortcut's ability to connect distant neighborhoods and make them dynamically more similar. However, a more detailed analysis is necessary for a quantitative understanding of a shortcut's effect on the particular type of synchrony that presages global extinction in this system.

Nevertheless, a decrease in the mean transient time T as a function of increasing shortcut length s can be explained in part by the decrease in characteristic path length l caused by the shortcut. Figure 3.2 shows the clear reduction in characteristic path length l as the length of the shortcut is increased. A shortcut that spans just a few nodes changes the characteristic path length l only a little, while a shortcut that halves the system shortens the path length by 25 percent.

Though a qualitative explanation of the decreasing trend in Fig. 3.1 has been made, the shortcuts actual effect on the system is not so simple. The increase in the average transient time T for small shortcut lengths ($s < 0.15$) cannot be explained. Furthermore, for any

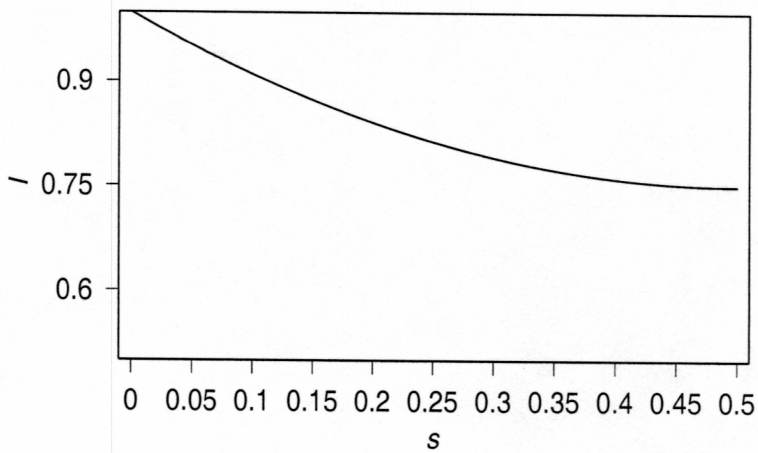

Figure 3.2. **Relative characteristic path length l as a function of shortcut length** s. l is given as a fraction of the path length in a system with no shortcut ($s = 0$).

value of s the transient time for some members of the ensemble was increased from that of the control case while for others it was decreased. Figure 3.3 gives information about this distribution. The solid curve shows the percentage of the ensemble whose transient time was decreased relative to the control case while the dashed curve shows the percentage whose transient times were increased. So, even for a shortcut length of $s = 0.5$ where the characteristic path length l is reduced by 25 percent, there exist a few simulations for which the transient time is actually increased in the presence of the shortcut.

These counterintuitive results suggest that at least one process other than the shortcut's reduction of characteristic path length governs its effect on the system's dynamics. Chapter 4 explores these other processes by taking a more detailed look at the effect of added shortcuts on the local dynamics of a system.

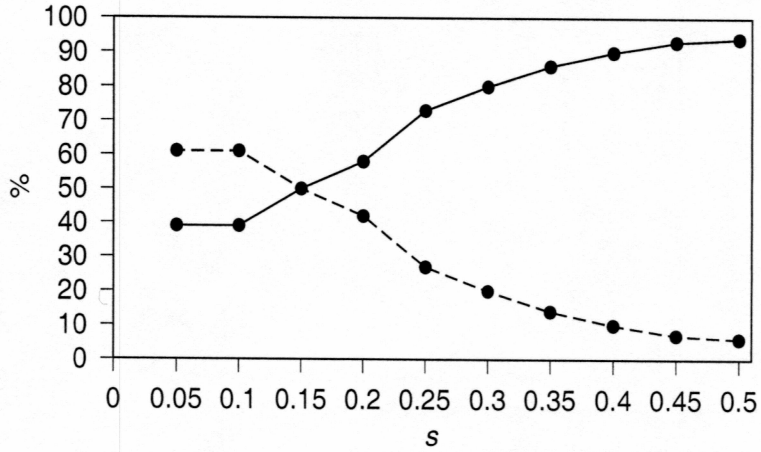

Figure 3.3. **Percentage of systems with transient times decreased (solid line) and increased (dashed line) relative to the control case** ($s = 0$)**.** The average transient times for this ensemble of systems are pictured in Fig. 3.1. The sytem's parameters are fully listed there.

Chapter 4

Local dynamics in the vicinity of a shortcut

An added shortcut's ability to decrease the average path length between nodes in a network does not explain the increase in the transient time of spatiotemporal chaos due to nearby shortcuts seen in Chap. 3. An understanding of this requires a detailed examination of the influence of added shortcuts on the local dynamics of the system.

4.1 The local consequences of one shortcut

A single shortcut was added to the regularly connected dynamical network as in Eqn. (2.5). It follows from Eqn. (2.5) that the perturbation generated by the shortcut becomes more important when the gradient between the linked nodes (m and n) increases. The gradient between the two shortcut nodes is largest when one node is within a locally extinct region while the other is in a dynamical (non-extinct) region. Figure 4.1(a) shows a sample of the spatiotemporal dynamics resulting from a shortcut in this extreme situation.

The shortcut does not become evident in Fig. 4.1(a) before the onset of the local extinction nor while both ends of the shortcut are inside the extinct region. The gradient between the two shortcut nodes is still too small for there to be a visible effect in the spatiotemporal dynamics of the system. An interface forms when the invading predator B reaches the right end of the shortcut and the two shortcut nodes are no longer both within the extinct re-

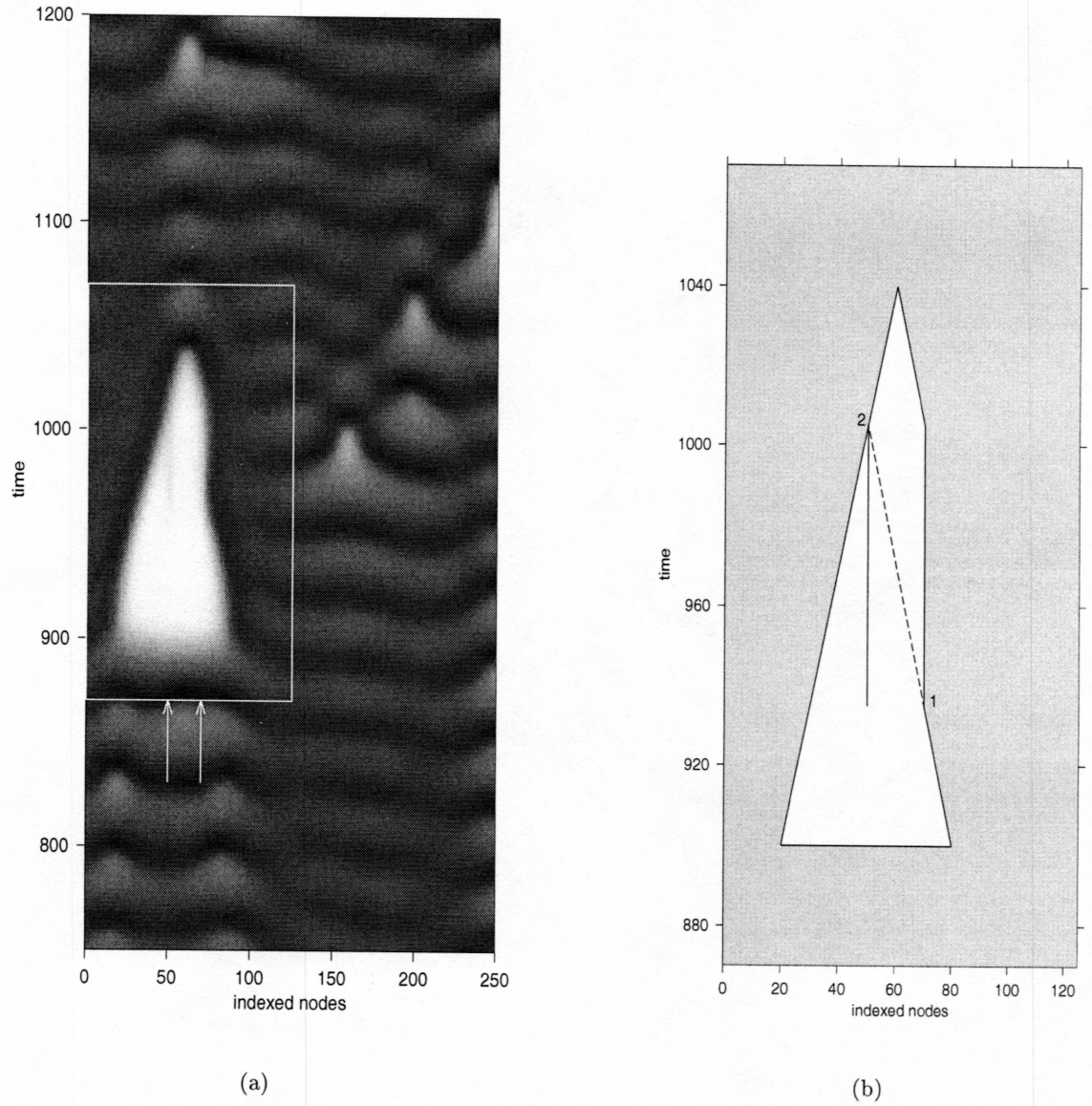

Figure 4.1. **Spatiotemporal dynamics of resource concentration a in the presence of an interface.** (a) A connection has been added between nodes 50 and 70 as marked. The system has $N = 400$ nodes, only a portion is shown here. Other numerical and system parameters are the same as used for Fig. 2.3. (b) Sketch of a local extinction in the presence of an interface. The dashed line indicates how the local extinction would evolve in the absence of the interface. The interface forms at point (1) and deteriorates at the time corresponding to point (2).

gion. This is in contrast with the evolution of a local extinction in the absence of a shortcut where the predator continues to invade from both sides (Fig 2.7). The interface prevents the recovery of the extinction from the right until the predator, invading from the other side, reaches the left end of the shortcut. The two ends, then, are no longer in dynamically different regions and the gradient between them is reduced. The interface disappears and the predator B invades from both sides of the local extinction.

The details of the interface are sketched out in Fig. 4.1(b). The dashed line shows how the local extinction would evolve in the absence of a shortcut. At point (1) the gradient between the two nodes becomes sufficient for the formation of the interface. The interface persists until the left hand edge of the shortcut is no longer within the extinct region at point (2). The gradient between the shortcut nodes is no longer sufficient to maintain the interface and the system evolves as it would in the absence of the shortcut.

Note that the interface causes the local extinction to last for longer than it would have in the regularly connected system. Already this suggests an explanation for the increased transient times in Chap. 3. Super-critical species concentrations at the boundaries of the local extinction prevent a global extinction [8]. The interface, by increasing the duration of local extinctions in the system, delays global extinction.

Figures 4.2 and 4.3 show concentration profiles for the predator B at successive moments in time surrounding the formation and deterioration of the interface. The first profile at time $t = 980$ in Fig. 4.2 occurs just before the interface's formation. Both ends of the shortcut are inside the locally extinct region and the gradient between them is close to zero. The shortcut is not visibly evident in this first profile. In the next profile at time $t = 960$ the predator B has invaded from the right. The right end of the shortcut is no longer inside the local extinction and there is a non-negligible gradient between the shortcut's two ends. The shortcut nodes are visible in this profile as the two cusps in the concentration of B. In the third profile at time $t = 980$ the cusps continue to be evident. The shortcut's left end is still within the local extinction so the gradient between the two nodes remains sufficient for the maintenance of the interface. The predator B's invasion from the right has been essentially halted.

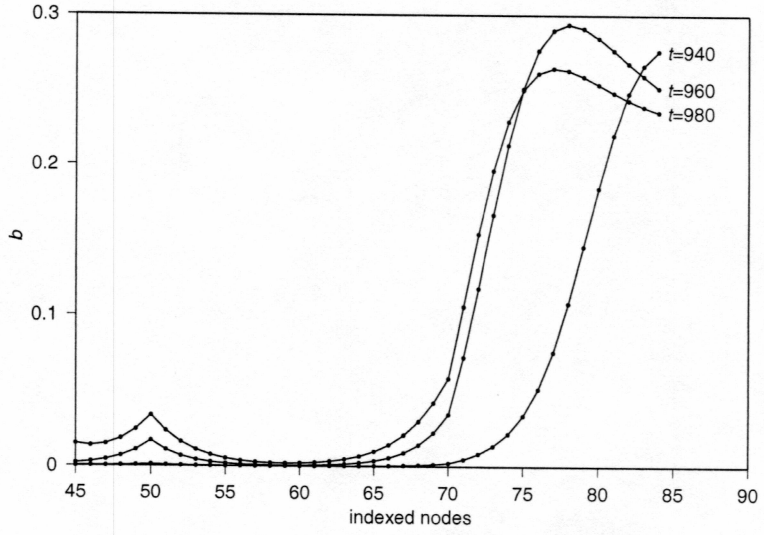

Figure 4.2. **Successive concentration profiles for species B in the vicinity of a forming interface corresponding to Fig. 4.1(a).** The connection has been added between nodes 50 and 70.

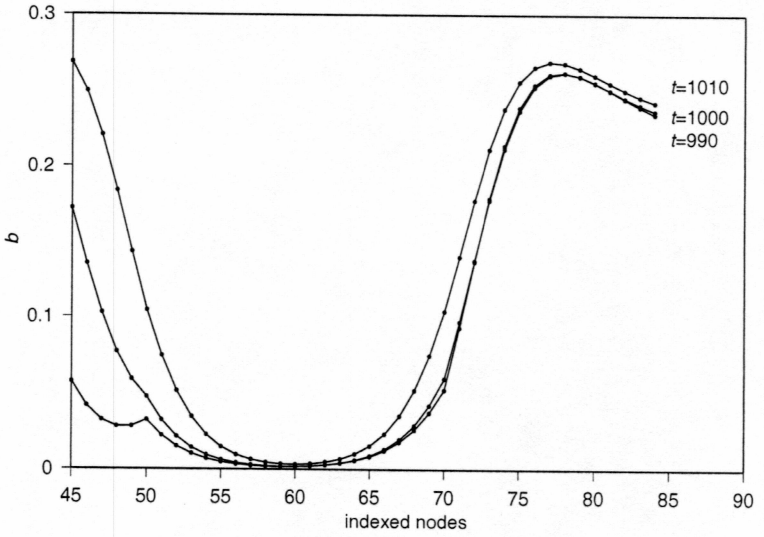

Figure 4.3. **Successive concentration profiles for species B in the vicinity of a deteriorating interface corresponding to Fig. 4.1(a).** The connection has been added between nodes 50 and 70.

Figure 4.3 shows the process in reverse as the interface deteriorates. In the first profile at time $t = 990$ the invading predator has almost reached the left hand side of the shortcut, though not quite. There is still an evident gradient between the two nodes, the cusps are still visible, and the predator species still has not invaded from the right across the interface. By the time of the next profile at time $t = 1000$ the predator has reached the left end of the shortcut. The two ends of the shortcut are no longer in different dynamical regions. The gradient between the shortcut nodes is reduced and the cusps are no longer visible. In the last profile at time t=1010 neither shortcut node is within the extinct region, and the added connection has no visible effect. The interface has deteriorated and the predator species has invaded from both sides of the local extinction.

The spatiotemporal dynamics in Fig. 4.1(a) and the concentration profiles in Figs. 4.2 and 4.3 indicate that an interface forms when one end of the shortcut is in the interior of an extinct region (the left end in Fig. 4.1(a)) while the shortcut's other end is simultaneously just outside the local extinction (the right end in Fig. 4.1(a)). Why, though, does this prevent invasion of the predator species?

The profiles in Figs. 4.2 and 4.3 along with the excitable nature of nodal dynamics in this system (see Fig. 2.1) provide the answer. With node m (left end of shortcut) in an extinct region where $b = 0$ while node n (right end of shortcut) is not, the gradient in Eqn. 2.5 has a sufficient negative value to ensure that the concentration of B at node n stays below the excitation threshold. Regardless of the influx of species B from neighboring nodes into the right end of the shortcut, the added connection drains so much of it that the node stays sub-critical and unable to perturb its extinct neighbor away from the stable steady state. Any predator invading across the interface must pass through the drained shortcut node n, and since that node cannot transmit enough predator to repopulate the extinct region, the boundary is preserved.

A necessary condition for the formation of an interface in the vicinity of a shortcut is a sufficient negative gradient at one of the shortcut's two ends. Figure 4.4 shows how the distance between the two trajectories in phase space, $\Delta = \sqrt{(a_m - a_n)^2 + (b_m - b_n)^2}$, changes in time for the spatiotemporal dynamics depicted in Fig. 4.1(a). The value of Δ is proportional to the magnitude of the gradient between the two connected sites. At the onset of local extinction, at time $t \approx 875$, Δ drops to zero signaling the synchronization

of the trajectories and their approach to the extinct state. The formation of the interface corresponds to Δ increasing at time $t \approx 950$. The interface itself corresponds to the top portion of the hump in Δ between time $t \approx 960$ and $t \approx 990$, and its deterioration, to Δ again dropping at time $t \approx 1010$. Compare the "knee" in Fig. 4.4 with the times for the formation and deterioration of the interface as shown in Figs. 4.2 and 4.3.

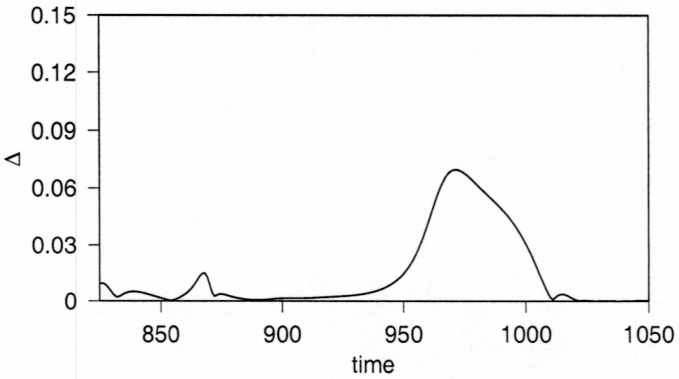

Figure 4.4. **Trajectory difference Δ between shortcut nodes nodes as a function of time.** Nodes are $m = 50$ and $n = 70$ in Fig. 4.1(a).

Figure 4.5 shows the phase portrait for the two shortcut nodes. The temporary existence of the interface is reflected by a small loop in the trajectories which do not occur at nodes in the regularly connected network (Fig. 2.3).

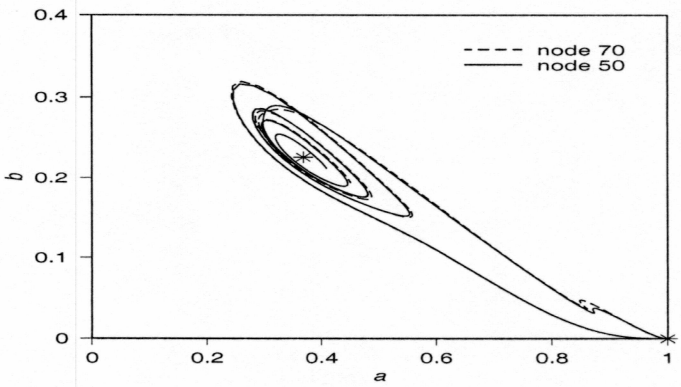

Figure 4.5. **Phase portrait for trajectories at shortcut nodes.** solid line corresponds to $m = 50$ in Fig. 4.1(a) and the dashed line to$m = 50$. Only the portion of the trajectories between time $t = 750$ and $t = 1050$ is shown.

The negative gradient required for the formation of an interface occurs when one end

of the shortcut be experiencing a local extinction, while the other is still in a dynamical region. The dynamical region does not have to be just on the edge of the extinction for this phenomenon to occur as demonstrated in Fig. 4.6. In this instance the condition for interface formation is met at the very onset of the local extinction. The interface forms well outside the local extinction so that there are nodes with super-critical concentrations of the predator B between the interface and the edge of the extinction and the invasion proceeds uninterrupted.

Figure 4.7 shows the concentration profiles of the predator species B corresponding to the interface depicted in Fig. 4.6. The first profile at time $t = 885$ occurs immediately prior to the formation of the interface. Already there is enough of a gradient between the shortcut nodes for cusps to be visible in the profile. The next two profiles at times $t = 900$ and $t = 930$ occur during the lifetime of the interface. Because of the super-critical concentration between shortcut nodes, the predator B is able to invade the locally extinct region from the right even though the interface is still evident. The propagating excitation wave front between the two cusps from time $t = 900$ to time $t = 930$ is shown Fig. 4.7. This is in contrast with the concentration profiles for an interface just at the local extinction's edge in Figs. 4.2 and 4.3 where no predator concentration propagates into the extinct region from the side with the interface.

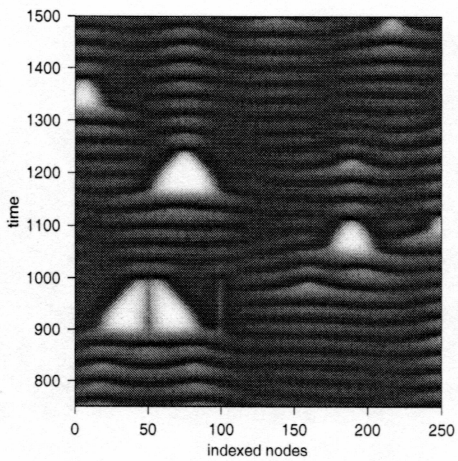

Figure 4.6. **Spatiotemporal dynamics of resource concentration a in the presence of an interface.** A connection has been added between nodes 50 and 95. The system has $N = 400$ nodes, only a portion is shown here. Numerical and system parameters are the same as used for Fig. 2.3.

The interface is paralleled with a strip of elevated predator concentration that forms inside the extinction. Though this is clearly evident in Fig. 4.6 the predator transmitted via the shortcut into the extinct region does not constitute a super-critical perturbation. Figure 4.8 shows an instance where the influx of predator through the shortcut does. An interface does briefly form, however, it is not self sustaining. The predator species B enters the extinction through the shortcut and stages an invasion from the inside.

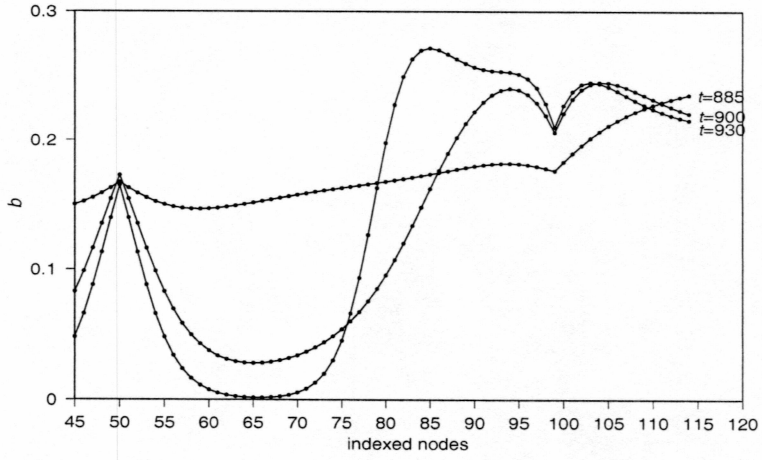

Figure 4.7. **Successive concentration profiles for species B in the vicinity of a forming interface corresponding to Fig. 4.6.** A connection has been added between nodes 50 and 95.

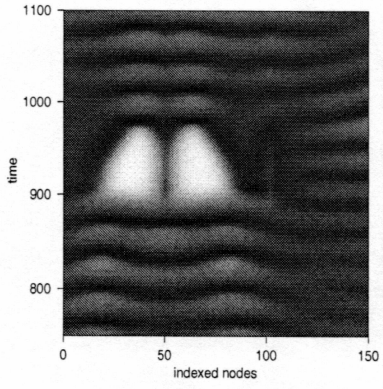

Figure 4.8. **Spatiotemporal dynamics of resource concentration a in the presence of an interface.** A connection has been added between nodes 50 and 101. The system has $N = 400$ nodes, only a portion is shown here. Numerical and system parameters are the same as used for Fig. 2.3.

4.2 The local consequences of two shortcuts

The interface caused by one shortcut can create a barrier interrupting the flow of predator B throughout the medium (Fig. 4.1(a)). The spatiotemporal dynamics shown in Fig. 4.9 shows a persistent local extinction (or *stripe*) created when two shortcuts have been added to an otherwise regularly connected network. The two shortcuts each create an interface blocking off one side of the local extinction.

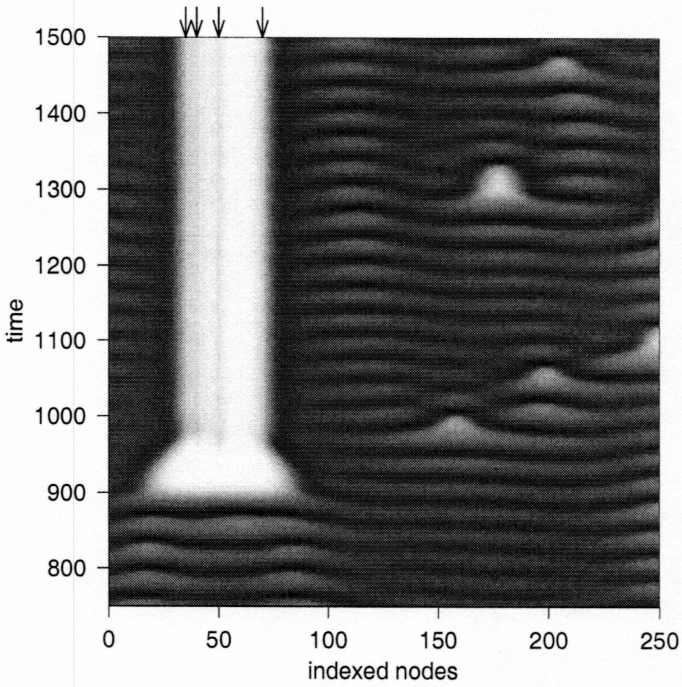

Figure 4.9. **Spatiotemporal dynamics of resource concentration a in the presence of two interfaces.** A connection has been added between nodes 30 and 45 and nodes 50 and 70 as marked. The system has $N = 400$ nodes, only a portion is shown here. Numerical and system parameters are the same as used for Fig. 2.1.

Since the predator species is not permitted to invade from either side, one end of both shortcuts is always in an extinct region while the other is in a dynamical region and the necessary condition for the two interfaces is perpetually sustained. The consequence of this phenomenon is profound. The persistent local extinction, or stripe, prevents the network from ever globally synchronizing. The global extinction inevitable in a regularly connected network is not possible with the addition of two shortcuts. The spatiotemporal chaos is no

longer transient, but asymptotic.

Figure 4.10 shows the concentration profiles for the predator B at the formation of one of the two interfaces. Comparing this figure to the profiles in Fig. 4.2 indicates that this interface forms just as it does when there is only one shortcut.

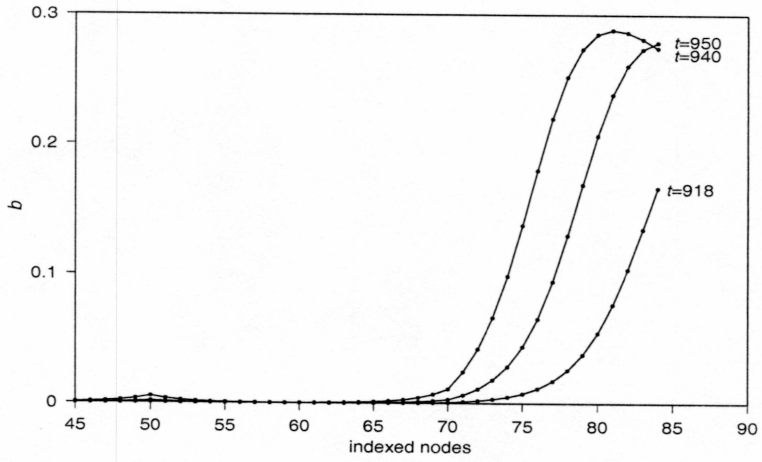

Figure 4.10. **Successive concentration profiles for species B in the vicinity of a forming interface corresponding to Fig. 4.9.** A connection has been added between nodes 50 and 70.

The permanence of the stripe allows some aspects of the interface to be explored more fully than when its lifetime is limited. Figure 4.11 shows the distance between the trajectories Δ for one of the shortcuts. As in the presence of a single shortcut (Fig. 4.4) the onset of local extinction corresponds to a decrease in Δ and the formation of the interface occurs as Δ rises. Instead of peaking and falling, though, Δ settles into oscillations about a fixed value. In the phase portrait of the two nodes (Fig. 4.12) the onset of local extinction followed by the formation and persistence of the interface is reflected as the two trajectories first make an excursion to the stable extinct state followed by an asymptotic approach to another point in phase space. This point corresponds to a coupling-induced shifted stable steady state [11]. The motion around this shifted state echoes the oscillation about the unstable focus (see Eqn. 2.3) of the neighboring trajectories. Compare these fixed points to the small loops executed by the two shortcut trajectories in the presence of a single interface (Fig. 4.5) where the interfaces existed only temporarily.

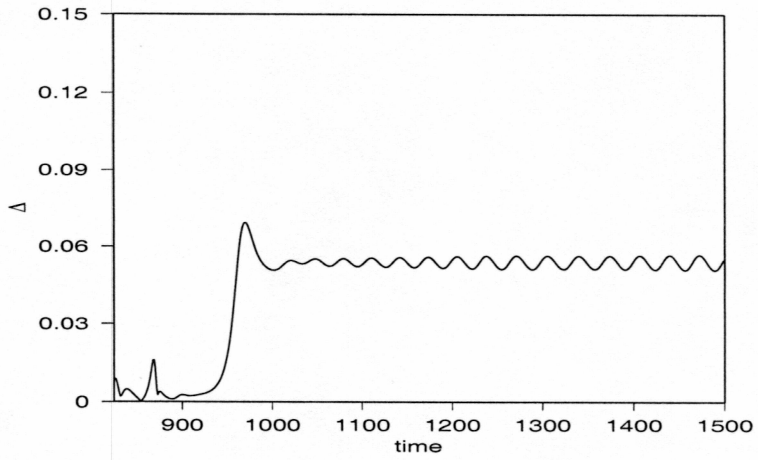

Figure 4.11. **Trajectory difference Δ between shortcut nodes as a function of time corresponding to Fig. 4.9.**

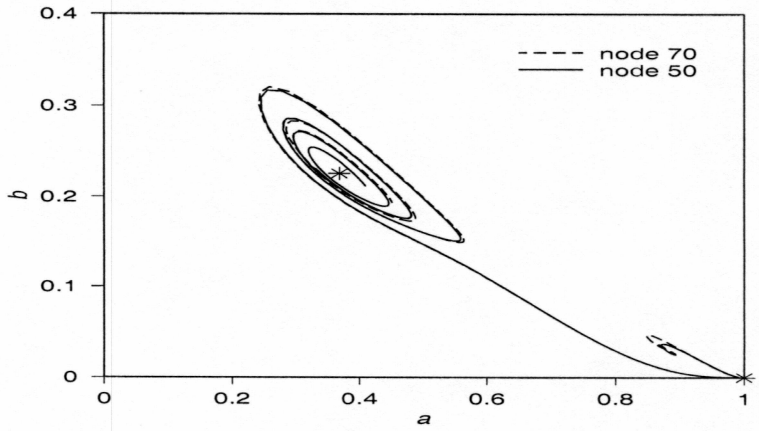

Figure 4.12. **Phase portrait for trajectories at shortcut nodes.** The solid line corresponds to $m = 50$ in Fig 4.9 and the dashed line to $n = 70$. Only the portion of the trajectories between times $t = 750$ and $t = 1500$ is shown.

4.3 Summary

Interfaces are caused when a shortcut connects an extinct region to a dynamical region. Singly, these interfaces extend the lifetime of local extinctions thus forestalling the global extinction. In a pair, these interfaces can effectively wall off an extinct region preventing

invasion from the predator species. This persistent local extinction (or stripe) prevents the system from ever reaching the globally extinct state.

These phenomena demonstrate that only a very few shortcuts are required to have a profound effect on the dynamics of the system. Just two shortcuts can transform transient spatiotemporal chaos to asymptotic.

Chapter 5

Conclusion

The interaction between the nodal dynamics and spatial coupling in a regularly connected ring network gives rise to transient spatiotemporal chaos. The dynamical collapse is preceded by a highly synchronous state. To gain insight into the relationship of the network's topology on this emergent chaotic dynamics and its ultimate collapse the regular network was modified by the addition of distant shortcuts. Following are the main results of these studies:

- The addition of a single shortcut to the regular ring network can hasten or delay the collapse of spatiotemporal chaos. If the added shortcut spans nodes whose separation approaches 50 percent of the ring, the average transient time for a set of random initial conditions is clearly reduced. For shortcuts spanning nodes that are likely to be part of a single local dynamical collapse however, the average transient time is increased.

- On the local level, when the shortcut connects a dynamical region to one experiencing local dynamical collapse, an interface forms. Via the interface the shortcut delays the recovery of the collapsed region. Since global collapse cannot occur when part of the system is in a locally collapsed state, increasing the lifetime of local dynamical collapses is a means by which the shortcut can delay global collapse.

- Two shortcuts can each form an interface, one on either side of a region whose dynamics have collapsed. This pair of interfaces creates a persistent region of local collapse that prevents the system's dynamics from ever collapsing globally.

The statistical results obtained for a single shortcut's effect on transient times as well as the interface and persistent collapse phenomena suggest much additional research along these lines. In addition to increasing the duration of local collapses, it is possible that the shortcut also makes local collapse more likely. A simulation to determine how the frequency and size of local collapses changes with shortcut length might shed light on this question.

Comparing the transient time as a function of shortcut length to the size distribution for local collapses might yield insight into the operation of the shortcut on the local level. An interface forms when a shortcut spans part of a local collapse. It therefore seems probable that transient times would be more likely increased when the shortcut's length is on the same order as the most frequent size of local dynamical collapse.

Shortcuts act on a global level to enhance a system's synchronicity and so hasten its global dynamical collapse, while on the local level they can interrupt the synchrony of a neighborhood as in the formation of an interface or persistent local collapse. The competition between these two processes might be elucidated in a statistical study where both the number and size of the shortcuts are varied.

Beyond manipulations of the regularly connected ring, the effect of shortcuts on the dynamics of other network topologies might also be explored. It would be interesting to determine the robustness of the interface phenomenon when shortcuts are added to regular networks where nodes are connected to four nearest neighbors instead of two as in this study. These more connected networks could also provide a means to explore the consequences of breaking connections instead of just adding them.

Today we are placing more stress on the connected systems of the natural world than ever before, while at the same time we depend on man-made networks for almost every aspect of modern life. Understanding the complex relationship between a network's structure and its dynamics is becoming ever more crucial. It is hoped that the studies presented in this thesis provide some tiny step toward achieving this understanding.

Bibliography

[1] Steven H. Strogatz. Exploring complex networks. *Nature*, 410:268–276, 2001. and other refernces therein.

[2] F Qi, Z Hou, and H Xin. Ordering chaos by random shortcuts. *Physical Review Letters*, 91(6):0641021–4, 2003.

[3] DJ Watts and SH Strogatz. Collective dynamics of small-world networks. *Nature*, 393:440–442, 1998.

[4] Rober C. Hilborn. *Chaos and Nonlinear Dynamics: an introduction for scientists and engineers, second edition.* Oxford University Press, Oxford ox2 6dp, 2000.

[5] Steven H. Strogatz. *Nonlinear Dynamics and Chaos: with applications to physics, biology, chemistry and engineering.* Perseus Books Group, Cambridge, Massachusetts, 2001.

[6] P Gray and SK Scott. Autocatalytic reactions in the isolated, continuous stirred tank reactor. *Chemical Engineering Science*, 39:1087–1097, 1984.

[7] JH Merkin, V Petrov, SK Scott, and K Showalter. Wave-induced chemical chaos. *Physical Review Letters*, 76(3):546–549, 1996.

[8] R Wackerbauer and K Showalter. The collapse of spatiotemporal chaos. *Physical Review Letters*, 91(17):1741031–4, 2003.

[9] K. McCann and P. Yodzis. *American Naturalist*, 144:873, 1994.

[10] L.Shulenburger, Y.-CH. Lai, T. Yalcinkaya, and R.D. Holt. *Physics Letters A*, 260:873, 1999.

[11] R Wackerbauer. *The Collapse of Spatiotemporal Chaos.* Talk at Dynamics Days, Tempe, Arizona, January, 2003.